

Deciphering Ξ^- capture events in light emulsion nuclei

Eliahu Friedman^{1,*} and Avraham Gal^{1,**}

¹Racah Institute of Physics, The Hebrew University, Jerusalem 9190401, Israel

Abstract. We recently showed that all five KEK and J-PARC uniquely assigned two-body $\Xi^- + {}^A Z \rightarrow {}^A_\Lambda Z' + {}^A_\Lambda Z''$ capture events in CNO light emulsion nuclei are consistent with Coulomb-assisted $1p_{\Xi^-}$ nuclear states in a Ξ^- -nuclear potential of nuclear-matter depth $V_{\Xi} \gtrsim 20$ MeV [1]. Here we argue that the recently reported ${}^{14}\text{N}$ capture events named KINKA and IRRAWADDY are more likely $1p_{\Xi^0-{}^{14}\text{C}}$ nuclear states [2] than $1s_{\Xi^--{}^{14}\text{N}}$ states that would imply considerably smaller values of V_{Ξ} .

1 Introduction

The nuclear interactions of Ξ hyperons are poorly known [3, 4]. Because of the large momentum transfer in the standard (K^-, K^+) production reaction, induced by the two-body $K^- p \rightarrow K^+ \Xi^-$ strangeness exchange reaction, Ξ^- hyperons are produced dominantly in the quasi-free continuum region. No Ξ^- nor $\Lambda\Lambda$ nuclear bound states have ever been observed unambiguously in such experiments [5–7]. Nevertheless, an attractive Ξ^- -nuclear Woods-Saxon (WS) potential of depth $V_{\Xi} = 17 \pm 6$ MeV [8] was deduced recently from the ${}^9\text{Be}(K^-, K^+)$ quasi-free Ξ^- spectrum shape [7] shown in Fig. 1.

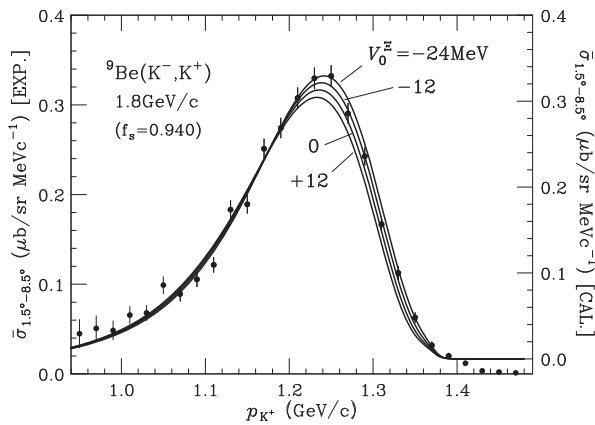


Figure 1. WS fit of the BNL-AGS E906 ${}^9\text{Be}(K^-, K^+)$ spectrum. Figure adapted from Ref. [8].

*Eliahu.Friedman@mail.huji.ac.il

**avragal@savion.huji.ac.il

A potential depth $V_{\Xi} = 17 \pm 6$ MeV is considerably larger than $V_{\Xi} \lesssim 10$ MeV deduced from strong-interaction models, e.g., HALQCD [9] (confirmed in $p\Xi^-$ femtoscopy [10]), EFT@NLO [11, 12] and RMF [13]. A notable exception is provided by versions ESC16*(A,B) of the latest Nijmegen model in which values of V_{Ξ} higher than 20 MeV arise [14]. However, these V_{Ξ} values get reduced by substantial ΞNN three-body contributions within the same ESC16* model.

Here we focus on Ξ nuclear constraints derived by observing Ξ^- capture events in exposures of light-emulsion CNO nuclei to the (K^-, K^+) reaction. A small fraction of the produced high-energy Ξ^- hyperons slows down in the emulsion, undergoing an Auger process to form high- n atomic states, and cascades down radiatively. Strong-interaction capture takes over atomic radiative cascade in a 3D atomic orbit bound by 126, 175, 231 keV in C, N, O, respectively, affected to less than 1 keV by the strong interaction [15]. Nevertheless, captures from a lower orbit have also been observed, as follows.

Table 1. Twin- Λ two-body Ξ^- capture events from KEK and J-PARC emulsion work. Deduced Ξ^- -nuclear binding energies B_{Ξ^-} are contrasted with purely Coulomb $2P$ atomic binding energies $B_{\Xi^-}^{2P}$.

Experiment	Event	${}^A Z$	${}^A Z' + {}^{A''} Z''$	B_{Ξ^-} (MeV)	$B_{\Xi^-}^{2P}$ (MeV)
KEK E176 [16]	10-09-06	${}^{12}\text{C}$	${}^4_{\Lambda}\text{H} + {}^9_{\Lambda}\text{Be}$	0.82 ± 0.17	0.285
KEK E176 [16]	13-11-14	${}^{12}\text{C}$	${}^4_{\Lambda}\text{H} + {}^9_{\Lambda}\text{Be}^*$	0.82 ± 0.14	0.285
KEK E176 [16]	14-03-35	${}^{14}\text{N}$	${}^3_{\Lambda}\text{H} + {}^{12}_{\Lambda}\text{B}$	1.18 ± 0.22	0.393
KEK E373 [17]	KISO	${}^{14}\text{N}$	${}^5_{\Lambda}\text{He} + {}^{10}_{\Lambda}\text{Be}^*$	1.03 ± 0.18	0.393
J-PARC E07 [18]	IBUKI	${}^{14}\text{N}$	${}^3_{\Lambda}\text{He} + {}^{10}_{\Lambda}\text{Be}$	1.27 ± 0.21	0.393

Listed in Table 1 are *all* two-body Ξ^- capture events $\Xi^- + {}^A Z \rightarrow {}^A_{\Lambda} Z' + {}^{A''}_{\Lambda} Z''$ to twin single- Λ hypernuclei uniquely identified in KEK and J-PARC light-nuclei emulsion K^- exposures [16–19]. Expecting Λ hyperons in $\Xi^- p \rightarrow \Lambda\Lambda$ capture to form a spin $S = 0$ $1s^2_{\Lambda}$ configuration, the initial Ξ^- hyperon and the proton on which it is captured must satisfy $l_{\Xi^-} = l_p$ [20], which for p -shell nuclear targets favors the choice $l_{\Xi^-} = 1$. Indeed, all the listed events are consistent with Ξ^- capture from Coulomb-assisted $1p_{\Xi^-}$ nuclear states, with $B_{\Xi^-}^{1P}$ larger by about 0.5 MeV than the corresponding $2P$ atomic binding energies $B_{\Xi^-}^{2P}$. Not listed in the table are multi-body capture events requiring undetected capture products, mostly neutrons, besides a pair of single- Λ hypernuclei. Two such events [19], KINKA (KEK-E373) and IRRAWADDY (J-PARC E07), correspond to a few MeV Ξ^- binding each, suggesting Ξ^- capture from $1s_{\Xi^-}$ nuclear states. Given that $1s_{\Xi^-}$ capture rates are of order 1% of the $1p_{\Xi^-}$ capture rates [20, 21], this poses a problem. Its likely resolution is discussed below.

2 Ξ nuclear optical potential

Ξ^- atomic and nuclear bound states in $N = Z$ nuclei such as ${}^{12}\text{C}$ and ${}^{14}\text{N}$ are calculated using a finite-size Coulomb potential $V_c^{\Xi^-}$, including vacuum-polarization terms, plus a ‘ $t\rho$ ’ optical potential V_{opt}^{Ξ} [1] where t is a spin-isospin averaged in-medium ΞN t -matrix and $\rho = \rho_n + \rho_p$ is a nuclear density normalized to the number of nucleons A . For V_{opt}^{Ξ} we adopt a form applied in Ref. [22] to V_{opt}^{Λ} :

$$V_{\text{opt}}^{\Xi}(r) = -\frac{2\pi}{\mu_{\Xi}} b_0^A(\rho) \rho(r), \quad b_0^A(\rho) = \frac{\text{Re } b_0^A}{1 + (3k_F/2\pi)\text{Re } b_0^A} + \text{Im } b_0. \quad (1)$$

Here μ_{Ξ} is the Ξ^- -nucleus reduced mass, $b_0^A(\rho)$ is an effective density-dependent ΞN isoscalar c.m. scattering amplitude, $b_0^A = (1 + \frac{A-1}{A} \frac{\mu_{\Xi}}{m_N}) b_0$ transforms b_0 from the ΞN c.m. frame to the Ξ -nucleus c.m. frame and k_F is the Fermi momentum associated with density ρ , $k_F^3 = 3\pi^2 \rho/2$.

Eq. (1) accounts for long-range Pauli correlations in ΞN in-medium multiple scatterings, starting at $\rho^{4/3}$ [23, 24]. Shorter-range correlation terms, arising in the present context from three-body ΞNN interactions, start at ρ^2 and are briefly discussed in the concluding section.

For $N = Z$ nuclear densities we assumed $\rho_n = \rho_p$ and identified the r.m.s. radius of ρ_p with that of the nuclear charge density. Folding reasonably chosen ΞN interaction ranges other than corresponding to the proton charge radius, varying the spatial form of the charge density, or introducing realistic differences between neutron and proton r.m.s. radii, made little difference: in ^{12}C , for example, all such calculated binding energies varied within a small fraction, about 0.03 MeV, of the ± 0.15 MeV uncertainty of $B_{\Xi}^{1p}(^{12}\text{C}) = 0.82 \pm 0.15$ MeV listed in Table 1.

For a given absorptivity of $\text{Im } b_0 = 0.01$ fm in Eq. (1), $B_{\Xi}^{1p}(^{12}\text{C}) = 0.82 \pm 0.15$ MeV was fitted by $\text{Re } b_0 = 0.495 \pm 0.030$ fm which in the limit $A \rightarrow \infty$ and $\rho(r) \rightarrow \rho_0 = 0.17$ fm $^{-3}$ leads to a depth value $V_{\Xi} = 21.2 \pm 0.7$ MeV in nuclear matter. This value is compatible with that derived from AGS-E906 as shown in Fig. 1 and is in agreement with values 21–24 MeV extracted from old emulsion events [25]. Disregarding Pauli correlations by setting $k_F = 0$ leads to almost 15% increase of the depth, whereas doubling $\text{Im } b_0$ increases the fitted $\text{Re } b_0$ by only 1% [1].

3 $1s_{\Xi^-}$ states in ^{14}N ?

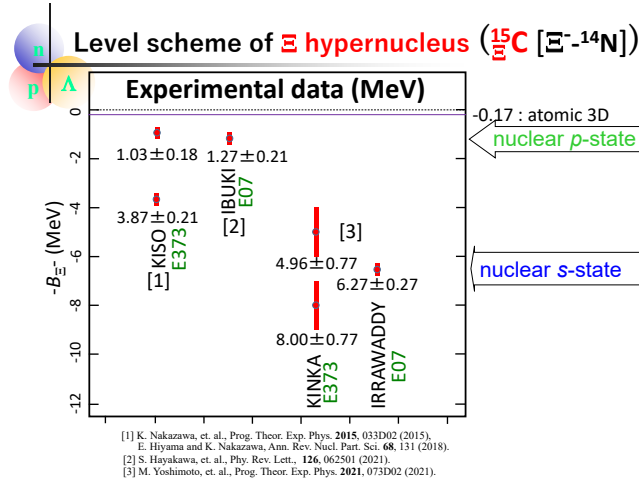


Figure 2. Binding energies of Ξ^- nuclear states in ^{14}N deduced from Ξ^- capture events identified by their twin- Λ hypernuclear decays in KEK-E373 and J-PARC E07 emulsion experiments. Figure provided by Dr. Kazuma Nakazawa, based on recent results from Refs. [17–19].

In addition to the KISO and IBUKI Ξ_{1p}^- twin- Λ capture events listed in Table 1, two new ^{14}N twin- Λ capture events were reported recently [19], KINKA from KEK E373 and IRRAWADDY from J-PARC E07, both assigned as Ξ_{1s}^- in Fig. 2. We note that $2P \rightarrow 1S$ radiative decay rates are of order 1% of $3D \rightarrow 2P$ radiative decay rates [20, 21] suggesting that Ξ^- capture from a nuclear Ξ_{1s}^- - ^{14}N state is suppressed to this order relative to capture from a nuclear Ξ_{1p}^- - ^{14}N state. Assigning a Ξ_{1s}^- - ^{14}N bound state to IRRAWADDY or to KINKA is therefore questionable.

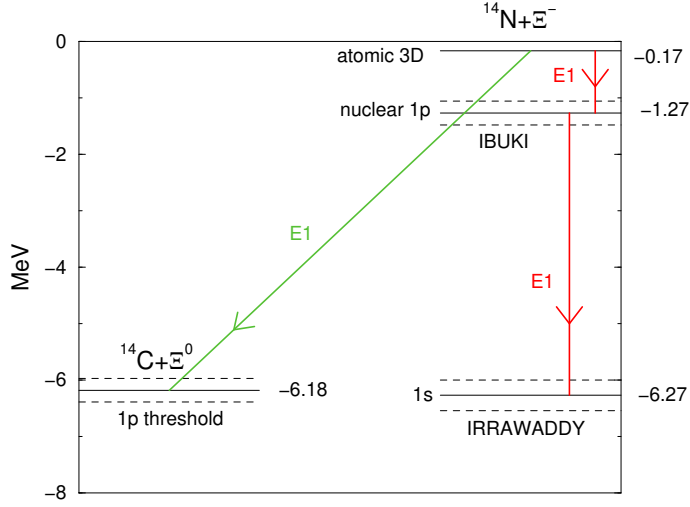


Figure 3. Level diagram of $\Xi^- - {}^{14}\text{N}$. Shown on the right are a $3D$ atomic state and $1p$, $1s$ nuclear states assigned, respectively, to E07 Ξ^- capture events IBUKI [18] and IRRAWADDY [19]. The $\Xi^0 + {}^{14}\text{C}$ threshold at -6.18 MeV is marked on the left. Electromagnetic $E1$ transitions deexciting the Ξ_{3D}^- atomic state to lower, slightly mixed together $\Xi^- - {}^{14}\text{N}$ and $\Xi_{1p}^0 - {}^{14}\text{C}$ nuclear states, are marked by red and green arrowed lines, respectively. A near-threshold $\Xi_{1p}^0 - {}^{14}\text{C}$ state on the left provides an alternative interpretation of IRRAWADDY [2].

It has been suggested by us recently [2] that IRRAWADDY is a near-threshold $\Xi_{1p}^0 - {}^{14}\text{C}$ bound state that has nothing to do with a $\Xi_{1s}^- - {}^{14}\text{N}$ bound state claimed by E07. The Coulomb potential's role in forming a *Coulomb assisted* $\Xi_{1p}^- - {}^{14}\text{N}$ nuclear bound state is replaced for $\Xi_{1p}^0 - {}^{14}\text{C}$ ($T = 1$) by adding a strong-interaction Lane term for isospin $T \neq 0$ nuclear cores in V_{opt} of Eq. (1). The sign and strength of this Lane term relative to $\text{Re } b_0$ were estimated in Ref. [2] from the sign and strength of V_τ relative to V_0 in the ΞN s -wave HALQCD underlying interaction [9]

$$V_{\Xi\text{N}} = V_0 + V_\sigma \vec{\sigma}_\Xi \cdot \vec{\sigma}_\text{N} + V_\tau \vec{\tau}_\Xi \cdot \vec{\tau}_\text{N} + V_{\sigma\tau} \vec{\sigma}_\Xi \cdot \vec{\sigma}_\text{N} \vec{\tau}_\Xi \cdot \vec{\tau}_\text{N}, \quad (2)$$

and were found sufficient to bind $\Xi_{1p}^0 - {}^{14}\text{C}$ near threshold, within the J-PARC E07 experimental uncertainty of IRRAWADDY, as shown in Fig. 3. This newly considered $\Xi_{1p}^0 - {}^{14}\text{C}$ and IBUKI's $\Xi_{1p}^- - {}^{14}\text{N}$ bound states get slightly mixed by $V_{\sigma\tau}$ of Eq. (2), sufficiently to make the ~ 6 MeV $E1$ radiative deexcitation of the $\Xi_{3D}^- - {}^{14}\text{N}$ atomic state to the dominantly $\Xi_{1p}^0 - {}^{14}\text{C}$ nuclear state as strong as to the ~ 1 MeV deexcitation to the IBUKI $\Xi_{1p}^- - {}^{14}\text{N}$ nuclear state. Assigning a $\Xi_{1p}^0 - {}^{14}\text{C}$ bound state structure to IRRAWADDY contrasts with viewing it as a $\Xi_{1s}^- - {}^{14}\text{N}$ state motivated largely by IRRAWADDY's binding energy of a few MeV.

It is worth recalling that in spite of limiting discussion to the fairly narrow IRRAWADDY, given that a KINKA+IRRAWADDY weighted average of $B_{\Xi^-} = 6.13 \pm 0.25$ MeV or 6.46 ± 0.25 MeV differs little from IRRAWADDY's own value of $B_{\Xi^-} = 6.27 \pm 0.27$ MeV, our arguments apply equally well to either one of KINKA's considerably broader versions.

Table 2. Input (underlined) and calculated mean values of Ξ^- binding energies in optical potential fits, plus resulting ΞN and ΞNN induced Ξ nuclear potential depths $V_{\Xi}^{(2)}$ and $V_{\Xi}^{(3)}$, respectively, at nuclear-matter density $\rho_0 = 0.17 \text{ fm}^{-3}$, and their correlated sum V_{Ξ} ; see text. Potentials and energies are given in MeV.

$B_{\Xi^-}^{1p} (^{12}\text{C})$	$B_{\Xi^-}^{1s} (^{14}\text{N})$	$B_{\Xi^-}^{1p} (^{14}\text{N})$	$V_{\Xi}^{(2)}$	$V_{\Xi}^{(3)}$	V_{Ξ}	$B_{\Xi^-}^{1s} (^{11}\text{B})$
<u>0.82</u>	11.79	1.94	21.2±0.7	–	21.2±0.7	9.00
0.32	<u>6.27</u>	0.52	13.6±0.4	–	13.6±0.4	4.20
<u>0.82</u>	<u>8.00</u>	<u>1.27</u>	26.4±2.6	–15.4±5.7	11.0±3.1	6.29
<u>0.82</u>	<u>6.27</u>	<u>1.27</u>	30.6±1.7	–28.2±3.9	2.4±2.2	5.15

4 Discussion

Some Ξ -nuclear scenarios are outlined in Table 2. Choosing $B_{\Xi^-}^{1p} = 0.82 \pm 0.15$ MeV for the two KEK-E176 ^{12}C events listed in Table 1 to fit the strength b_0 of the ΞN induced Ξ -nuclear attractive optical potential V_{opt}^{Ξ} in Eq. (1) results in several other Ξ^- nuclear binding energies listed in the first row. Choosing instead the J-PARC E07 ^{14}N IRRAWADDY event [19] with $B_{\Xi^-}^{1s} = 6.27 \pm 0.27$ MeV as input results in values listed in the second row of the table. Clearly, these two sets of results differ strongly for the $\Xi_{1s}^- - ^{11}\text{B}$ binding energies discussed below and for the Ξ -nuclear attractive potential depths $V_{\Xi}^{(2)}$. Regarding the Coulomb assisted Ξ_{1p}^- bound states, we note that the $\Xi_{1p}^- - ^{12}\text{C}$ capture event constrained by IRRAWADDY in the second row comes out less than 40 keV bound with respect to a purely Coulomb $2P$ atomic state, strongly disagreeing with 540 ± 150 keV deduced from the KEK E176 events [16] underlined in the first row.

The next two rows in Table 2 report on fitting *two* Ξ -nucleus interaction parameters, b_0 for the ΞN induced attractive V_{opt}^{Ξ} , Eq. (1), and B_0 for a ΞNN induced potential term

$$\delta V_{\text{opt}}^{\Xi}(r) = \frac{2\pi}{\mu_{\Xi}} \left(1 + \frac{A-2}{A} \frac{\mu_{\Xi}}{2m_N} \right) B_0 \frac{\rho^2(r)}{\rho_0} \quad (3)$$

introduced in our recent work on the content of the Λ -nuclear optical potential [22]. Both ^{12}C and ^{14}N Ξ_{1p}^- bound states are used for input, along with KINKA's higher-binding option in the third row or IRRAWADDY in the fourth row for $B_{\Xi^-}^{1s} (^{14}\text{N})$ to allow for some variation. Both fits are acceptable, $\chi^2 < 1$, with a substantial ΞNN induced repulsive $\delta V_{\text{opt}}^{\Xi}$ almost doubling its strength as $B_{\Xi^-}^{1s} (^{14}\text{N})$ input is decreased from 8.00 ± 0.77 MeV in the third row to 6.27 ± 0.27 MeV in the fourth row. We note that the ΞN induced potential $V_{\Xi}^{(2)}$ depth values obtained when $\delta V_{\text{opt}}^{\Xi}$ is introduced increase farther away from the considerably smaller values of $V_{\Xi}^{(2)}$ obtained in recent theoretical models [9, 11], while the total depth V_{Ξ} decreases farther away from $V_{\Xi} = 17 \pm 6$ MeV suggested by the $^9\text{Be}(K^-, K^+)$ spectrum in Fig. 1.

The solution proposed here to the difficulty of interpreting IRRAWADDY as a Ξ_{1s}^- bound state in ^{14}N is by pointing out that it could correspond to a $\Xi_{1p}^0 - ^{14}\text{C}$ bound state, something that cannot occur kinematically in the other light-emulsion nuclei ^{12}C and ^{16}O . Given that in this nuclear mass range capture rates from $1s_{\Xi^-}$ states are estimated to be two orders of magnitude below capture rates from $1p_{\Xi^-}$ states [20, 21], our $\Xi_{1p}^0 - ^{14}\text{C}$ assignment addresses satisfactorily the capture rate hierarchy.

Regarding $1s_{\Xi^-}$ states, J-PARC E70 $^{12}\text{C}(K^-, K^+) ^{12}\text{Be}$ experiment with record 2 MeV FWHM simulated resolution [26], following an earlier experiment E05 with 5.4 MeV FWHM resolution [27], aims particularly to observe $1s_{\Xi^-} - ^{11}\text{B}$ signals. The last column in Table 2 lists a wide range of predicted $B_{\Xi^-}^{1s} (^{11}\text{B})$ values depending on which Ξ^- -capture data are accepted. Corrections of order 0.5 MeV are likely from the three spin-isospin ΞN terms in Eq. (2).

Acknowledgments

One of us (A.G.) thanks the organizers of MESON2023 in Krakow for support and hospitality. This work is part of a project funded by the EU Horizon 2020 Research & Innovation Programme under grant agreement 824093.

References

- [1] E. Friedman, A. Gal, Phys. Lett. B **820**, 136555 (2021)
- [2] E. Friedman, A. Gal, Phys. Lett. B **837**, 137640 (2023)
- [3] A. Gal, E.V. Hungerford, D.J. Millener, Rev. Mod. Phys. **88**, 035004 (2016)
- [4] E. Hiyama, K. Nakazawa, Annu. Rev. Nucl. Part. Sci. **68**, 131 (2018)
- [5] T. Fukuda *et al.* (KEK E224), Phys. Rev. C **58**, 1306 (1998)
- [6] P. Khaustov *et al.* (BNL-AGS E885), Phys. Rev. C **61** 054603 (2000)
- [7] J.K. Ahn *et al.* (BNL-AGS E906), Phys. Rev. Lett. **87**, 132504 (2001)
- [8] T. Harada, Y. Hirabayashi, Phys. Rev. C **103**, 024605 (2021)
- [9] K. Sasaki *et al.* (HAL QCD), Nucl. Phys. A **998**, 121737 (2020)
- [10] S. Acharya *et al.* (ALICE), Phys. Rev. Lett. **123**, 112002 (2019)
- [11] J. Haidenbauer, U.-G. Meißner, Eur. Phys. J. A **55**, 23 (2019)
- [12] M. Kohn, Phys. Rev. C **100**, 024313 (2019)
- [13] T. Gaitanos, A. Choroziou, Nucl. Phys. A **1008**, 122153 (2021)
- [14] M.M. Nagels, Th.A. Rijken, Y. Yamamoto, Phys. Rev. C **102**, 054003 (2020)
(See in particular Tables XXI, XXIV for models ESC16*(A,B), respectively)
- [15] C.J. Batty, E. Friedman, A. Gal, Phys. Rev. C **59**, 295 (1999)
- [16] S. Aoki *et al.* (KEK E176), Nucl. Phys. A **828**, 191 (2009)
- [17] H. Nakazawa *et al.* (KEK E373), Prog. Theor. Exp. Phys. **2015**, 033D02 (2015)
- [18] S.H. Hayakawa *et al.* (J-PARC E07), Phys. Rev. Lett. **126**, 062501 (2021)
- [19] M. Yoshimoto *et al.* (J-PARC E07), Prog. Theor. Exp. Phys. **2021**, 073D02 (2021)
- [20] D. Zhu, C.B. Dover, A. Gal, M. May, Phys. Rev. Lett. **67**, 2268 (1991)
- [21] T. Koike, JPS Conf. Proc. **17**, 033011 (2017)
- [22] E. Friedman, A. Gal, Nucl. Phys. A **1039**, 122725 (2023)
- [23] C.B. Dover, J. Hüfner, R.H. Lemmer, Ann. Phys. (NY) **66**, 248 (1971)
- [24] T. Waas, M. Rho, W. Weise, Nucl. Phys. A **617**, 449 (1997)
- [25] C.B. Dover, A. Gal, Ann. Phys. (NY) **146**, 309 (1983)
- [26] T. Gogami *et al.*, EPJ Web of Conf. **271**, 11002 (2022), in particular Fig. 2
- [27] T. Gogami *et al.*, J. Phys. Conf. Ser. **1643**, 012133 (2020), in particular Fig. 2